Supplementary Information

# $T_1$-$T_2$ Dual-Modal Magnetic Resonance Contrast-Enhanced Imaging for Rat Liver Fibrosis Stage

Fulin Lu[a,b], Liang Du[a], Wei Chen[a], Hai Jiang[a], Chenwu Yang[a], Yu Pu[a], Jun Wu[a], Jiang Zhu[a], Tianwu Chen[a], Xiaoming Zhang[a], Changqiang Wu[a*]

[a] Medical Imaging Key Laboratory of Sichuan Province and School of Medical Imaging, Affiliated Hospital of North Sichuan Medical College, Nanchong 637000, China.

[b] Department of Radiology, Sichuan Academy of Medical Sciences and Sichuan Provincial People's Hospital, University of Electronic Science and Technology of China, Chengdu 610072, China.

Correspondence should be addressed to Changqiang Wu; wucq1984@nsmc.edu.cn

## 1. Synthesis of Ultrafine PEGylated Superparamagnetic Iron Oxide Nanocrystal

SPIO nanocrystals were synthesized by high-temperature thermal decomposition of iron acetylacetonate, and the ultrafine size of SPIO nanoparticles were composed by controlling the reaction heating conditions. $Fe(acac)_3$ (353 mg), 1,2-hexadecanediol (1.435 g), oleic acid (0.951 g), oleamine (1 g), diphenyl ether (10 mL) were mixed and magnetically stirred. The mixture were slowly heat to 200 °C for 30 min and then, under a blanket of nitrogen, heated to reflux (265 °C) for another 30 min. The black-brown mixture was cooled to room temperature by removing the heat source, and obtain organic phase monodisperse SPIO nanoparticles (SPIO@OA). After that, SPIO nanocrystals were transferred to aqueous phase by ligand exchange reaction with the sodium citrate. Citric acid was dissolved in water (70 mL), sodium hydroxide was added to adjust the pH to 7.4, then added hexane (70 mL), acetone (110 mL) and SPIO@OA heaed to 70 °C for 48 h to obtain the aqueous phase citric acid coated SPIO nanoparticles (SPIO@CA). Finally, dopamine polyethylene glycol (PEG-DA, with the same molar mass of SPIO@CA) was dissolved in water (10 mL) reacting with SPIO@CA at 40 °C for 24 h to obtain ultrafine SPIO@PEG nanoparticles.

## 2. Ultrafine SPIO@PEG characterization

1~2 μL of the SPIO@OA and SPIO@PEG solution were diluted and droped onto the TEM special copper mesh membrane, and evaporate it at room temperature for TEM and SAED detections. Similarly, 1 mL of SPIO@OA and SPIO@PEG samples were seperately diluted to a quartz dish for DLS testing, and the measurement was repeated 3 times at 25 °C. 1~2 mg powdered SPIO@OA, SPIO@CA and SPIO@PEG samples were used for FTIR testing, and the test wavenumber range is 4000~500 $cm^{-1}$.

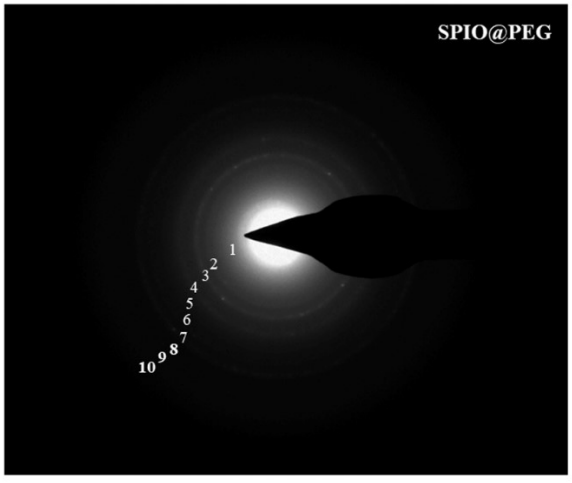


| ring | hkl | d | $Fe_3O_4$ |
|---|---|---|---|
| 1 | 111 | 4.71 | 4.86 |
| 2 | 220 | 3.02 | 2.97 |
| 3 | 311 | 2.61 | 2.53 |
| 4 | 400 | 2.14 | 2.10 |
| 5 | 422 | 1.73 | 1.71 |
| 6 | 511 | 1.67 | 1.62 |
| 7 | 440 | 1.53 | 1.48 |
| 8 | 620 | 1.34 | 1.33 |
| 9 | 533 | 1.26 | 1.28 |
| 10 | 444 | 1.14 | 1.21 |

Figure S1. SAED patter of SPIO@PEG nanoparticles and Measured Lattice Spacing

values (d) which are obtained from the ring and hkl indexes compared with the known lattice spacing of $Fe_3O_4$ from the PDF database.

## 3. $T_1$ value measured by variable flip angle (VFA) method.

$T_1$ mapping images were acquired using a series of liver acquisition volume acceleration (LAVA), with five flip angles 3°, 6°, 9°, 12°, and 15°.$T_1$ mapping images were transferred to MATLAB. $T_1$ maps were generated by MATLAB using the VFA method. $T_1$ relaxation times were calculated as follows: The signal intensity "S" was determined by the equilibrium magnetization "$M_0$," longitudinal relaxation "$T_1$," repetition time "TR," and flip angle "α," giving rise to the following:

$$S = M_0 * \frac{\sin\alpha * \left(1 - E_1\right) * E_2}{1 - E_1 * \cos\alpha} \quad (1)$$

Where $E_1$ = exp(-TR/T1), and $E_2$ = exp(-TE/$T_2$* ) can be normally ignored when TE<<$T_2$*. Equation (1) can be reformulated into a linear form:

$$\frac{S}{\sin\alpha} = E_1 * \frac{S}{\tan\alpha} + M_0 * \left(1 - E_1\right) \quad (2)$$

Since TR is constant, different flip angles can establish a series of equations. If we consider $\frac{S}{tan\alpha}$ as X, and $\frac{S}{sin\alpha}$ as Y, those equations will have an intercept of $M_0$* (1-$E_1$), and a slope of $E_1$, which could easily be solved with linear least square fit.

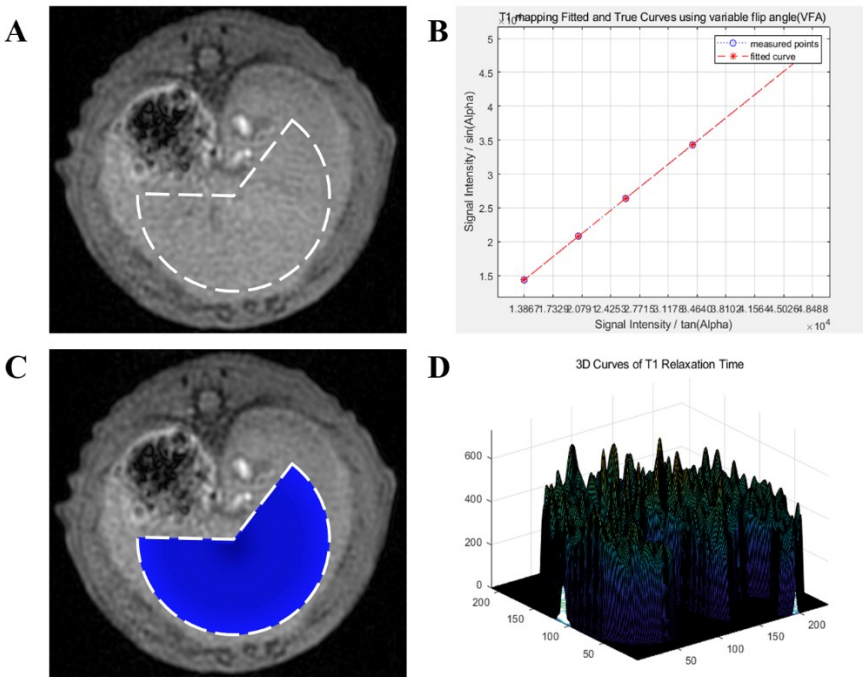


Figure S2. Illustration of $T_1$ value measurements. (A) regine of interest (ROI) which is drawn on the MR image. (B) $T_1$ linear least square fit measured by varible flip angle method. (C) Based on the $T_1$ value measurements and the ROI were colored by MATLAB (version 9.7 (R2019b), Mathworks, USA). (D) $T_1$ value distribution curve in the regine of ROI.

## 4. $T_2$ value measured by variable echo time curve fitting model.

The monoexponential function model was used to fit the $T_2$ signal versus echo time (TE) decay curve.

$$S = S_0 \exp( - TE*R_2) \quad (3)$$

Where S is the measured signal, S0 is the initial signal amplitude, and $R_2 = 1/T_2$ is the effective transverse relaxation rate. In this study, the parameter of the sequences were TE = 8, 16, 24, 31, 39, 47, 55, 63 ms, TR = 1.2 s, FOV = 80 mm × 80 mm, slice thickness = 2.0 mm, slice spacing = 0.6 mm, and flip angle = 90°. And the $T_2$ vaule of the liver were calculated by the fiting linear function. All simulations were implemented by MATLAB (version 9.7 (R2019b), Mathworks, USA).

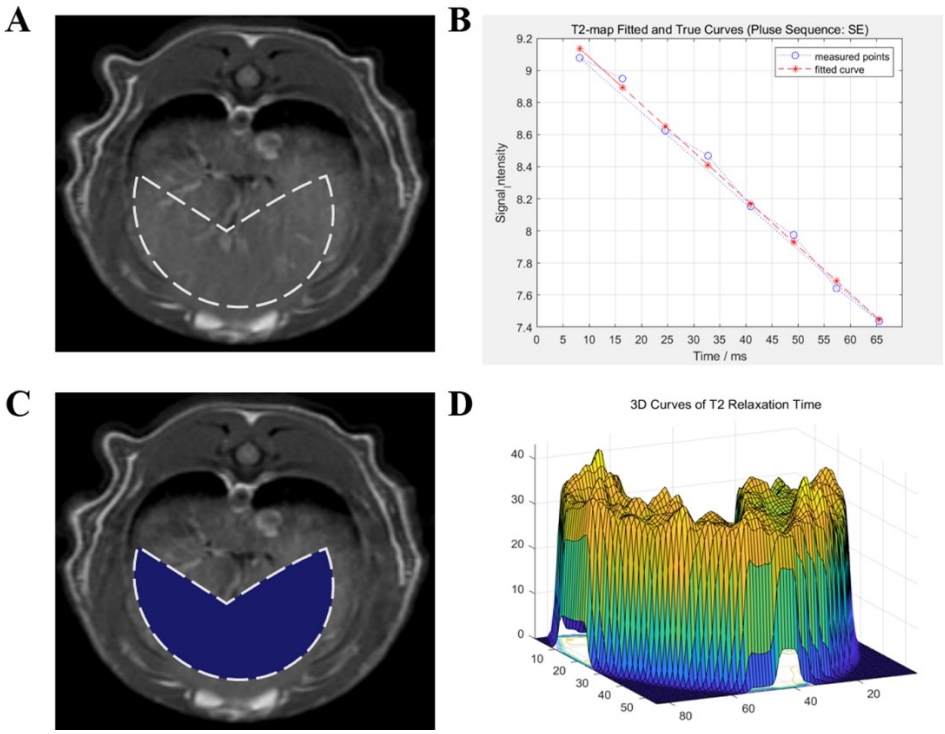


Figure S3. Illustration of $T_2$ value measurements. (A) regine of interest (ROI) which is drawn on the MR image. (B) $T_2$ linear least square fit measured by varible flip angle method. (C) Based on the $T_2$ value measurements and the ROI were colored by MATLAB. (D) $T_2$ value distribution curve in the regine of ROI.

## 5. Image fusion procession.

Based on the $T_1$ mapping and $T_2$ mapping results, we further investigated the image fusion of the $T_1$-$T_2$ dual-mode image. We separately measured the $T_1$ relaxation time and $T_2$ relaxation time of the same pixel on ROI the MR images and compared the values with the threshold, if both the $T_1$ and $T_2$ values were higher than the threshold the pixel will be output as positive pixel in red and depicted at the $T_2$ weighted MR images. Otherwise, the pixel will be output as negative pixel in blue.

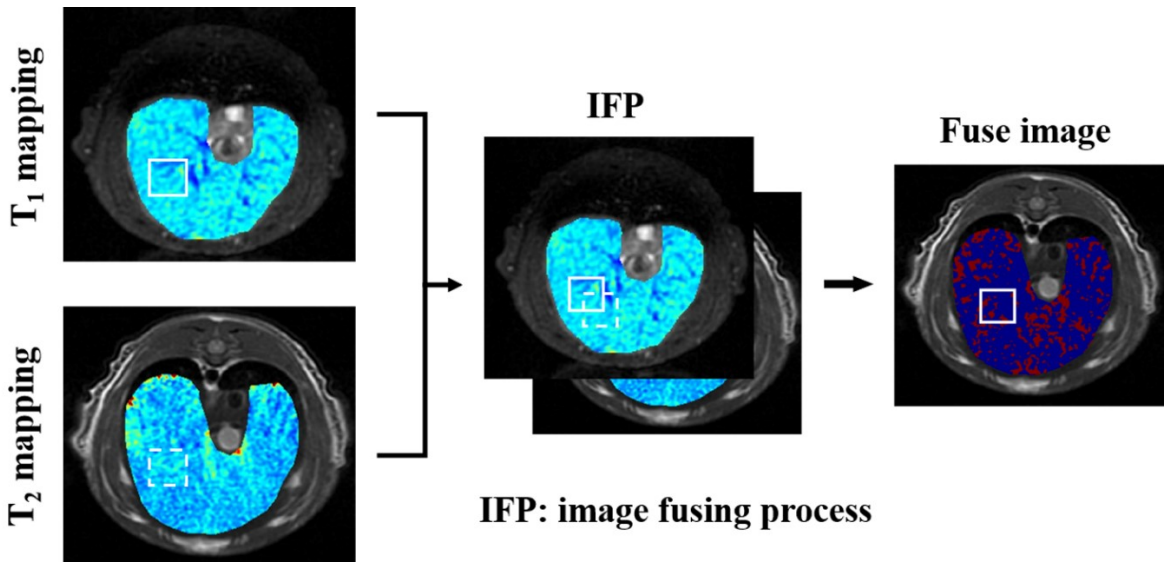


Figure S4. Illustration of image fusion procession. The ROI were placed on the liver in both $T_1$ and $T_2$ mapping images.